THE JOURNAL OF PHYSICAL CHEMISTRY A

Article

pubs.acs.org/JPCA

IPPP-CLOPPA Analysis of the Influence of the Methylation on the Potential Energy and the Molecular Polarizability of the Hydrogen Bonds in the Cytosine−Guanine Base Pair

Claudia G. Giribet* and Martín C. Ruiz de Azúa

Facultad de Ciencias Exactas y Naturales, Departamento de Física, Universidad de Buenos Aires, 1428 Buenos Aires, Argentina
Instituto de Física de Buenos Aires (IFIBA), CONICET, Universidad de Buenos Aires, 1428 Buenos Aires, Argentina

ABSTRACT: The IPPP-CLOPPA method is applied to investigate the influence of a methyl group on the energy of the hydrogen bonds and the potential energy curve of the bridge protons in model compounds, which mimic the methylated and unmethylated cytosine-guanine base pairs. On the same grounds, this influence on the polarizability of the intermolecular hydrogen bonds of these compounds is also addressed, in order to determine whether this linear response property provides a significant proof of the electronic mechanisms that affect the stabilization of the hydrogen bonds. Results obtained show that the methyl electronic system delocalizes on the hydrogen bond region, and changes of these intermolecular hydrogen bonds are due to this effect of delocalization.

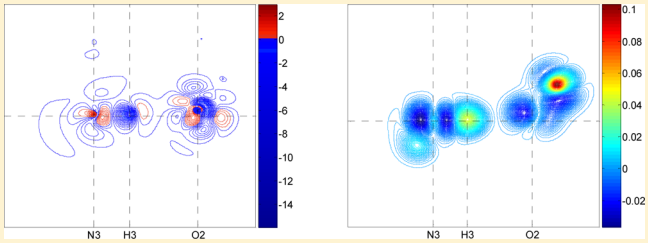

INTRODUCTION

Hydrogen bonding has received considerable attention, both from experimental and theoretical points of view, due to its fundamental role in many physical, chemical, and biochemical phenomena. In particular, the influence of methylation or other substituents[1] on the hydrogen bonds (HBs) of the DNA base pairs is a subject of particular interest, since a long time ago.[2−4] It is well-known that methylation in genomic DNA is a common epigenetic modification that is involved in many biological processes and it is commonly related to the silence of gene expression and point mutations,[5−11] including carcinogenesis.[12−17] Although epigenetic methylation follows different patterns, one the most common occurs at the C(5) site of cytosine of CpG islands in DNA.[7] Since methylation is a natural method of gene silencing, this process may cause changes in the strength and characteristics of the hydrogen bonding interactions involved in the base pairs.[7] However, in general, despite the many studies on the effects of cytosine methylation on gene expression, the underlying mechanisms are still poorly understood.[11] Severin et al. found that methylation could regulate gene expression through changing DNA mechanical properties.[12] However, to our knowledge, there has been little work connecting electronic interactions calculations with bioinformatics analyses.[18] Therefore, elucidating the effects of the C5-methylation of cytosine on the HBs and the electronic mechanisms operating on it would be a valuable step toward understanding the factors that control these biological processes. In particular, the question arises whether, and how, methylation stabilizes the cytosine-guanine base pair, and, therefore, the double helix.[5] To this purpose, perhaps the most valid criterion for evaluating the HB strength, and, therefore, the stability of the base pair, should be the analysis of the potential interaction energy of the proton in the HB region.[1,10,22] However, it must be taken into account that more subtle features of the interaction between the methyl group and the HBs could not be detected by means of a first-order property like the interaction energy, but, as it was already demonstrated,[23] more and further information on the involved electronic mechanisms can be obtained by the analysis of a second-order response property like the molecular polarizability.

Several attempts to deal with the energy of hydrogen bonds in DNA base pairs are found in literature, from different perspectives and applying many diverse tools,[1,7,9,18−24] as its experimental evaluation is a difficult task.[20] Many of them found that the stability of H-bonding originates in the Hartree−Fock component of interaction energy, which means that the interaction is mostly of electrostatic origin,[1,7,20,21] the other contributions being of much less importance.[19−21] Several methods were used to estimate this interaction energy: the supermolecule method, combined with the Bader's AIM (atoms-in-molecules) approach,[9] analysis of the methylation on the energetics of stacked base pairs,[18] the variation-perturbation energy decomposition scheme,[19,21] and the EFP2 (effective fragment potential) method.[22]

The aim of this work is, therefore, to address the aforementioned issues by means of (i) the calculation of the energy of the HB fragments, in order to assess the influence of the methyl system on them, and (ii) the analysis of the molecular polarizability of the HB moieties, and its changes

Received: October 5, 2016
Revised: March 27, 2017
Published: March 28, 2017

DOI: 10.1021/acs.jpca.6b10059
J. Phys. Chem. A 2017, 121, 2960−2970

when the compound is methylated, in order to determine whether this property can give information about the electronic mechanisms that affect the stabilization of the hydrogen bonds.

The question of whether there is a connection between the strength of the DNA base pairs HBs and a response property like the molecular polarizability was dealt with before,[20] but it was concluded that this second-order property is more likely correlated with stacking ability than with HBs stability.[17,25] In spite of this conclusion, in previous papers[23,26−28] it was shown that the decomposition of the molecular polarizability into local contributions arising from different molecular fragments provides insight into the underlying interactions inside the electronic cloud, information that cannot be obtained from the bulk property. Thus, this kind of analysis seems to be useful to assess the influence of the Me system in the HB region.

The IPPP-CLOPPA (Inner Projections of the Polarization Propagator-Contributions from Localized Orbitals within the Polarization Propagator Approach) technique[29−31] has proven to be a convenient method to deal with these issues, as it was intended to identify the electronic mechanisms operating in a given phenomenon in terms of localized molecular orbitals (LMOs). Although it was implemented for the theoretical analysis of NMR spin−spin couplings[32−36] and the static molecular polarizability tensor,[25−28] the same scheme can be used for any second-order molecular property. Additionally, more recently, the same idea of defining a molecular fragment with LMOs was applied for calculating first-order properties; in particular, the energy associated with a molecular fragment.[23]

The present paper is organized as follows. First, a brief account of the IPPP-CLOPPA method is presented, and applied to estimate the energy of a fragment and the interaction energy within the fragment in terms of LMOs; in particular, it is applied to calculate the HB energy and the potential energy of the proton in the HB moiety. The same method is also applied to calculate the molecular polarizability tensor of a molecular fragment. Numerical results of the analysis of the molecular polarizability and the energy of the intermolecular HBs of model compounds that mimic the main characteristics of the cytosine-guanine (CG) and C(5) methylated cytosine-guanine (C5mCG) bases pairs are presented in the "Results and Discussion" section. Results obtained are compared with the corresponding values calculated for the CG and C5mCG base pairs in order to validate the performed analysis. Interesting features, which complement and give a new insight into previous studies, are found, which are summarized in the Conclusions section.

METHODS

The IPPP-CLOPPA Method. The CLOPPA and the IPPP methods[29−31] are useful tools to identify the underlying electronic mechanisms that define a given phenomenon inside a molecule or a molecular fragment, in terms of localized molecular orbitals (LMOs). They can be applied to any second-order response property at the RPA level of approximation.[23,26−28] Most recently, the same ideas were implemented for calculating first order properties, in particular, the energy of molecular fragments.[23] In this work, the analysis of this latter property, as well as the molecular polarizability tensor are relevant, so the main ideas of the methods applied to these properties are outlined here, for the sake of comprehension.

Energy of a Molecular Fragment. The total energy of a molecular fragment can be evaluated by projecting the Fock operator onto the subset of occupied LMOs that define the fragment, plus the nuclear potential energy, that is,

$$E_{\mathrm{frag}} = \sum_{i\in \mathrm{frag}} \left[2\sum_{k}^{N/2} \langle i|k\rangle \varepsilon_k \langle k|i\rangle - \sum_{j\in \mathrm{frag}} (2\langle ij|ij\rangle - \langle ij|ji\rangle)\right] + \frac{1}{2}\sum_{n}^{M\in \mathrm{frag}} \sum_{m\neq n} V_{nm} \tag{1}$$

where subindices (i,j) designate those LMOs that span the molecular fragment, while k runs for canonical MOs; ε_k are orbital energies corresponding to canonical molecular orbitals, $\langle ij|ij\rangle$ and $\langle ij|ji\rangle$ stand for the Coulomb and exchange integrals, respectively, calculated between LMOs of the molecular fragment, $(n,m = 1,...,M)$ are the M nuclei of the chosen fragment, and V_{nm} represents the electrostatic interaction potential energy between nuclei. Although this form of defining the energy restricts the calculation to a particular fragment, it also takes into account the interaction of the fragment with the electrons of the rest of the molecule.

Likewise, the potential energy of the H proton in the HB moiety, $V_{\mathrm{HB}}(\mathrm{H})$, can be calculated as

$$V_{\mathrm{HB}}(\mathrm{H}) = \sum_{n}^{M\in \mathrm{HB}} V_{\mathrm{H}n} + \sum_{i\in \mathrm{HB}} \langle i|V_{\mathrm{He}^-}|i\rangle = V_{\mathrm{H,Nuc}} + V_{\mathrm{H,e}^-} \tag{2}$$

where the first sum includes the electrostatic interaction potential energy of the proton with the nuclei, $V_{\mathrm{H,Nuc}}$, and the second one, its interaction with the electrons of the fragment, $V_{\mathrm{H,e}^-}$.

The Molecular Polarizability Tensor. Within the polarization propagator (PP) formalism at the RPA level, the static polarizability tensor can be written as[37]

$$\vec{\vec{\alpha}} = -2\sum_{ia\le jb} {}^1P_{ia,jb}[\langle a^*|\vec{x}|i\rangle\langle b^*|\vec{x}|j\rangle + \langle b^*|\vec{x}|j\rangle\langle a^*|\vec{x}|i\rangle] \tag{3}$$

where i,j (a,b) indices stand for occupied i,j (vacant a^*,b^*) molecular orbitals (MOs) of a Hartree−Fock (HF) reference state, ${}^1P_{ia,jb} = -({}^1A-{}^1B)^{-1}_{ia,jb}$ is the singlet part of the PP matrix, connecting "virtual excitations" $i \rightarrow a^*$ and $j \rightarrow b^*$. Integrals $\langle a^*|\vec{x}|i\rangle$ and $\langle b^*|\vec{x}|j\rangle$ are the so-called "perturbators", the matrix elements of the dipole operator $\vec{x}$ between an occupied and a vacant MO.

In the CLOPPA method, the polarizability tensor $\vec{\vec{\alpha}}$ is rewritten in terms of LMOs, by applying to the PP matrix elements and to the perturbators convenient and consecutive unitary transformations from canonical HF MOs to occupied and vacant LMOs, separately, in such a way that the resultant LMOs represent chemical functions like bonds, lone pairs and atomic inner shells, and their corresponding "anti" LMOs (antibonds, antilone pairs, etc.). Here, the prefix "anti" followed by the name of an occupied LMO is used to designate those vacant orbitals localized using the same criteria as their occupied counterparts, and it indicates the spatial location of the vacant LMOs. The formal expression of $\vec{\vec{\alpha}}$ in terms of LMOs (eq 3) is not altered, but i,j indices now stand for occupied LMOs and a,b indices stand for vacant LMOs. However, the expression of the elements of the PP in terms of LMOs differs from their expression in terms of canonical MOs, when applying the above-mentioned unitary transformations.

DOI: 10.1021/acs.jpca.6b10059
J. Phys. Chem. A 2017, 121, 2960−2970

The *rs* Cartesian component of the polarizability tensor (*r,s* = *x,y,z*) arising from a chosen molecular fragment can be obtained by restricting the sum to the "local subspace",[25,27] i.e., the subset of LMOs that define this fragment:

$$\alpha^{L,rs}_{\mathrm{CLOPPA}} = -2 \sum_{ia \le jb}^{\mathrm{local}} {}^1P_{ia,jb}[\langle a^*|x_r|i\rangle\langle b^*|x_s|j\rangle + \langle b^*|x_r|j\rangle\langle a^*|x_s|i\rangle]$$

$$\alpha^{L,rs}_{\mathrm{CLOPPA}} = \sum_{ia \le jb}^{\mathrm{local}} \alpha^{rs}_{ia,jb} \quad (r, s = x, y, z) \tag{4}$$

Although the *i,a,j,b* LMOs involved belong to the local fragment, it must be noted that each $\alpha^{rs}_{ia,jb}$ term also contains the indirect influence of the whole molecule on the fragment, as the ${}^1P_{ia,jb}$ depends on all LMOs of the molecule. Within the IPPP method, the "strictly local" contribution of a local fragment, that is, the contribution that strictly arises from the chosen fragment, can be obtained, by "inner projecting" the PP matrix onto the local subspace.[29,30] This projected propagator ${}^1W$ is used in the calculation, instead of the whole PP matrix:

$$\alpha^{L,rs}_{\mathrm{IPPP}} = -2 \sum_{ia \le jb}^{\mathrm{local}} {}^1W_{ia,jb}[\langle a^*|x_r|i\rangle\langle b^*|x_s|j\rangle + \langle b^*|x_r|j\rangle\langle a|x_s|i\rangle]$$

$$\alpha^{L,rs}_{\mathrm{IPPP}} = \sum_{ia \le jb}^{\mathrm{local}} \alpha^{L,rs}_{ia,jb} \quad (r, s = x, y, z) \tag{5}$$

"Proper" LMO Polarizabilities and "Mutual" Polarizabilities. Within *ab initio* calculations, there are several vacant LMOs that can be ascribed to each type of local moiety. Therefore, the four-index terms appearing in eqs 4 and 5 are more conveniently defined as[25,27]

$$\alpha^{rs}_{ia,jb} = \sum_{\substack{\alpha \in 'a' \\ \beta \in 'b'}}^{\mathrm{local}} \alpha^{rs}_{i\alpha,j\beta} \tag{6}$$

where α (β) represent vacant LMOs of the a^* (b^*) type. Each term $\alpha^{rs}_{ia,jb}$ indicates to what extent the a^*-type vacant LMOs contribute to the polarization induced in the $|i\rangle$ occupied LMO by the effect of intramolecular interactions, when the $|j\rangle$ occupied LMO is coupled with the b^*-type vacant LMOs by the external field. Therefore, each term gives a measure of the efficiency of such involved LMOs in transmitting the polarization of the electronic cloud induced by the external perturbation.

In the same way, two-index contributions for a given pair of occupied LMOs *i* and *j* can be defined by summing over the whole set of vacant LMOs:[27]

$$\alpha^{rs}_{ij} = \sum_{a,b} \alpha^{rs}_{ia,jb} \tag{7}$$

As it was previously shown,[27] these terms can be interpreted as the *s* component of the induced dipole on the $|i\rangle$ occupied LMO (per unit field), due to the field created by the polarization of the $|j\rangle$ LMO in the presence of an external electric field $\vec{E}_r = E_r\hat{x}_r$:

$$\alpha^{rs}_{ij} = \frac{1}{E_r}[\langle \tilde{i}|x_s|\tilde{i}\rangle - \langle i|x_s|i\rangle] \tag{8}$$

where $|\tilde{i}\rangle$ is the modified occupied $|i\rangle$ LMO due to the polarization of the $|j\rangle$ LMO. Terms of this type are called "mutual polarizabilities".

In the same way, if $i = j$, eq 8 represents the *s* component of the dipole moment (per unit field) of the LMO $|i\rangle$ induced by the *r* component of the external field $\vec{E}$, i.e., the *rs* polarizability component of the occupied $|i\rangle$ LMO.[27] These α^{rs}_{ii} terms will be referred to as "proper LMO polarizabilities". Both mutual and LMO polarizabilities represent local properties within the molecule, and they provide a "local" picture of the distortion of the electronic system owing to an external field and, moreover, they give a quantitative idea of the "mobility" of the electrons on a certain molecular region. Therefore, this local description seems to be adequate to account for the effect of nonuniform electric fields on the molecular electronic distribution, such as the effect of the field of a given molecular group over another molecular fragment. In particular, if this field $\vec{E}$ does not vary considerably in the spatial region where the $|i\rangle$ LMO is localized, then the dipolar approximation can be applied, and the induced dipole moment of the $|i\rangle$ LMO can be evaluated in terms of the occupied LMOs polarizabilities as

$$\langle \tilde{i}|x_s|\tilde{i}\rangle - \langle i|x_s|i\rangle = E_r(\langle \vec{r}_o\rangle)\alpha^{rs}_{ii} \tag{9}$$

where the field is evaluated at an adequate middle site $\langle \vec{r}_o\rangle$ of the fragment.

RESULTS AND DISCUSSION

In order to investigate the methylation influence on the CG hydrogen bonds, the energy potential wells of the protons and the polarizability of the intermolecular hydrogen bonds of model compounds are analyzed. Taking into account that a qualitative more than a quantitative analysis is sought, these model compounds were chosen for the sake of simplicity, and they were constructed in such a way to retain the main characteristics of the electronic environment of the CG and C5mCG base pairs hydrogen bonds. Moreover, it is an interesting aim of this work to show how similar molecular fragments lead to similar qualitative and quantitative trends. In this regard, a comparison between some results obtained for the model compounds and the CG base pairs is also shown. The geometric structure of the CG base pair was optimized by means of the DALTON program[38] with a 6-31g(d,p)[39] basis set, considering that bond length and angle changes upon substitution were fairly negligible.[20] Then, the structure of the cytosine molecule, the three HBs, and their nearest surroundings were preserved, while the rest of the guanine molecule was simplified, keeping neutrality. The model compounds used and the numbering of the atoms are shown in Chart 1. Two different cases are considered: compound I, an H atom (H1) bonded to C5, and compound II, a methyl group bonded to C5. Calculations were performed by means of the SYSMO[40−42] program, at the RPA[37] level for the polarizabilities. CLOPPA and IPPP analyses of polarizabilities and electronic energy were carried out by means of a modified version of the SYSMO program.

The localization procedure was extensively explained previously,[27,34−36] therefore it is not commented on in this work. The notation used to identify occupied and vacant LMOs obtained by the localization procedure is depicted in Table 1. Only occupied and vacant LMOs localized in the HBs zones, the C−H1/C-Me moieties (see Chart 1) are considered, as the influence of these latter systems on the HBs is to be assessed.

DOI: 10.1021/acs.jpca.6b10059
J. Phys. Chem. A 2017, 121, 2960−2970

Chart 1. Geometric Structure of Cytosine−Guanine Base Pairs and Model Compounds

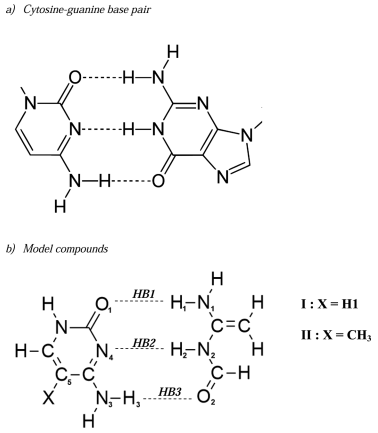

Table 1. Labeling of the LMOs

	occupied LMOs	vacant LMOs
(anti)inner shell of atom X	S(X)	S(X)*
σ-(anti)bond between X and Y	X−Y	X−Y*
π-(anti)bond between X and Y[a]	π(X−Y)	π(X−Y)*
(anti)Lone pair of atom X of μ (μ = σ,π) symmetry	LP_μ(X)	LP_μ(X)*
(anti)methyl group C−CH_3	Me	Me*
(anti)LMOs localized in the n (n = 1,2,3) hydrogen bond region	HBn[b]	HBn*[c]
σ-bridge vacant LMOs	-	HBσ*
π-bridge vacant LMOs	-	HBπ*

[a]When no atoms are indicated, it refers to the whole π system. [b]Includes D−H (where D is the donor atom), LP_μ(D), X−A (where A is the acceptor atom), π(X−A) and LP_μ(A); [c]Includes D−H*, LP_μ*(D), X−A*, LP_μ*(A), π(X−A)*, HBσ*, and HBπ*.

Unless explicitly stated, the vacant LMOs localized in each HB zone are joined together and indistinctly referred to as HB* LMOs, σ or π. As it was shown before,[34−36] they are physically significant in the hydrogen bond formation.

HB Energy Analysis: Influence of the Me Moiety. In Table 2, the Hartree−Fock and the MP2[43] (Møller−Plesset 2) contributions to the electronic energy for compounds I, II, CG, and C5meCG are displayed, in order to determine whether correlation effects are not negligible. The MP2 contribution is calculated with the DALTON[38] program. From this Table, it can be seen that the MP2 contribution represents only 0.31% of the total energy for all compounds considered, as can be expected taking into account that first-order properties are not quite as sensitive to correlation effects. Therefore, it can be concluded that RPA values are adequate for performing the present analysis. Obviously, it must be taken into account that total values corresponding to the model compounds can not be directly compared with those of the base pairs. However, the Table also shows that the energy difference, between model compounds and between base pairs, calculated with the RPA or SOPPA[43] schemes, are nearly the same.

Table 2. Comparison between the Correlation and the HF Contributions to the Total Energy for Model Compounds I and II, and CG and C5meCG[a]

	HF	MP2	%(MP2)[b]
I	−693.44559178	−2.15997520	0.31
II	−732.48056005	−2.31428077	0.31
Δ_{II-I}	−39.03496827	−0.15430557	0.39
CG	−932.08461971	−2.88720027	0.31
C5meCG	−971.11973747	−3.04147863	0.31
$\Delta_{C5meCG-CG}$	−39.03511776	−0.15427836	0.39

[a]All values in au. [b]Calculated as $(E_{MP2}*100)/(E_{HF} + E_{MP2})$.

In order to assess the influence of the Me moiety on the HBs, the potential energy curve of the proton in each of the HB fragments is calculated as in eq 2 along the line between both donor and acceptor atoms, including only the occupied LMOs of the fragment and (a) the C−H1 bond in compound I, and (b) the C−Me moiety in compound II. For the sake of simplicity, the C−Me moiety will be referred as the "Me group". Figures 1 and 2 depict the curves obtained in both cases for the three HBs, where the potential curves are plotted against the distance between the proton and its corresponding donor or acceptor atom, that belonging to the cytosine molecule. Several features are noteworthy. As it can be seen from Figure 1, the potential curves for the three HBs present several qualitative and quantitative differences in the case of compound I. Thus, HB3 and HB1 are quite similar heteronuclear asymmetric two-wells low-barrier hydrogen bonds, while HB2 is a homonuclear single-well one. However, it is worth noting that the interaction of the Me moiety with the proton yields significant changes in the potential energy of the three HBs. As it can be observed in Figure 2, a neat lowering of the potential energy is a common feature for the three HBs, whereas an increasing of the depth of the potential wells, mainly those which are closer to the Me group, can be observed for HB3 and HB1, and it is less significant for HB2. This effect is much more pronounced for HB3, for which there is a further deepening of the N donor well, most probably due to its closer proximity to the Me moiety. In spite of this last assertion, it is mostly interesting to observe that the interaction with the Me group affects HB1 in such a way that the potential well close to the acceptor O atom gets deeper than that near the donor N atom. This fact would suggest that the interaction of the Me group with the HB1 proton favors the bond of the proton with the acceptor O atom, instead of with the donor N one. In addition, a slight shift of the minima toward the position of the

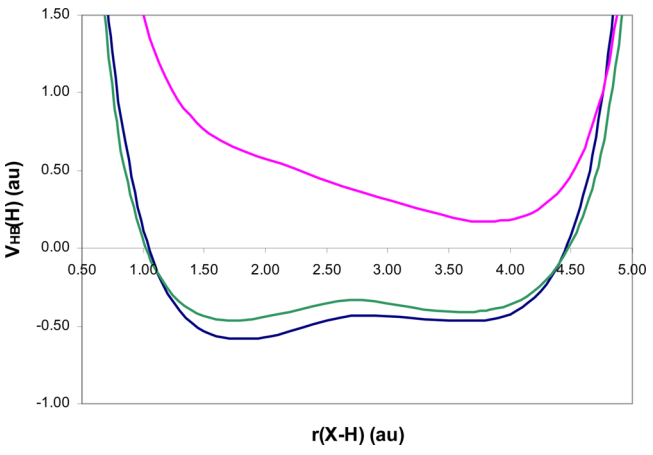

Figure 1. Potential energy for the protons in the hydrogen bonds of compound I, plotted against the distance between the proton and its corresponding donor or acceptor atom, that belonging to the cytosine molecule. Energy values are in au.

DOI: 10.1021/acs.jpca.6b10059
J. Phys. Chem. A 2017, 121, 2960−2970

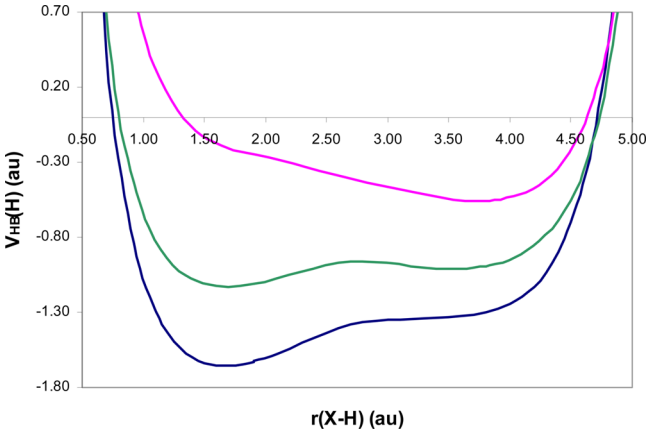

Figure 2. Potential energy for the protons in the hydrogen bonds of compound II, plotted against the distance between the proton and its corresponding donor or acceptor atom, that belonging to the cytosine molecule. Energy values are in au.

methyl group is observed for HB2 and HB3, due to the interaction of the proton with this group, stronger than with the C−H1 one. As it was pointed out,[44] the strongest heteronuclear HBs are highly asymmetric; therefore, it can be concluded that the interaction with the Me group contributes to further stabilize the bridge (most especially HB3), further confining the proton in one well. Figure 3 illustrates this trend, where the differences of the potential energies for the proton in the three HBs, between compounds II and I, are plotted. It is worth noting that this stabilization effect is due to the monoelectronic interaction energy between the proton and the electrons of the Me fragment, rather than a change of the interaction with the electrons of the HB zone. In fact, for example, for the equilibrium distance in HB3, the difference

$$\Delta V_{\mathrm{H,e^-}} = \sum_{i\in \mathrm{Me}} \langle i|V_{\mathrm{He^-}}|i\rangle - \sum_{i\in (C-H)} \langle i|V_{\mathrm{He^-}}|i\rangle = -1.0466 \text{ au}$$

accounts for almost the total difference

$$\Delta V_{\mathrm{HB}}(\mathrm{H}) = V_{\mathrm{HB}}(\mathrm{H, II}) - V_{\mathrm{HB}}(\mathrm{H, I}) = -1.0452 \text{ au}$$

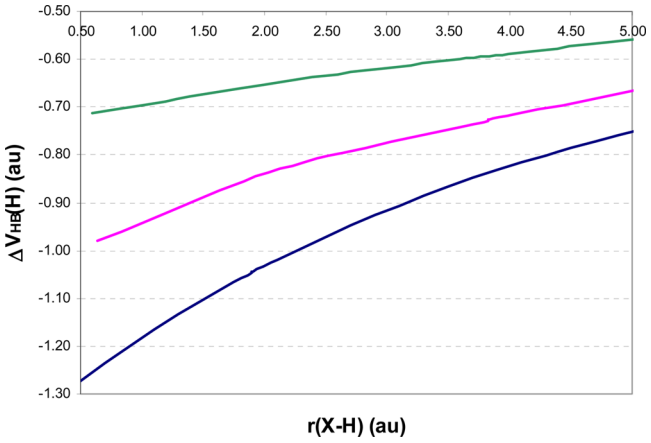

Figure 3. Potential energy difference for the protons in the hydrogen bonds between compound II and compound I, $\Delta V_{\mathrm{HB}}(\mathrm{H}) = V_{\mathrm{HB}}(\mathrm{H,II}) - V_{\mathrm{HB}}(\mathrm{H,I})$, plotted against the distance between the proton and its corresponding donor or acceptor atom, that belonging to the cytosine molecule. Energy values are in au.

a) $\Delta\rho_\sigma = \rho_\sigma(II) - \rho_\sigma(I)$

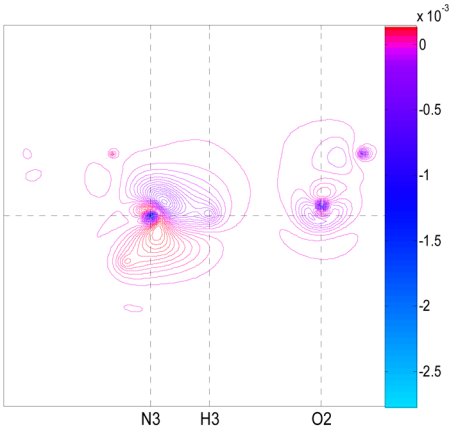

b) $\Delta\rho_\pi = \rho_\pi(II) - \rho_\pi(I)$

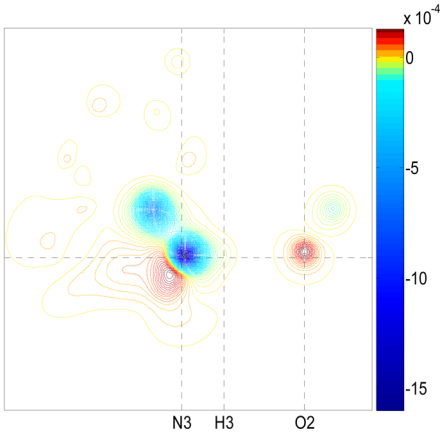

Figure 4. Difference between HB3 (a) σ, $\Delta\rho_\sigma$, and (b) π, $\Delta\rho_\pi$, electronic densities in compounds II and I. π electronic densities are calculated at 0.5 au from the molecular plane.

This fact might be indicative that the Me group alters the electronic density in the bridge, transferring charge to that zone. To illustrate this effect, Figure 4 depicts the differences between the HB3 σ (Figure 4a) and π (Figure 4b) electronic densities in compounds II and I (π electronic densities are calculated at 0.5 au from the molecular plane). It is observed that, due to the presence of the Me group, the σ electronic density is increased in the surroundings of the N−H3 bond, while decreasing in the O2 acceptor zone. On the other hand, it can be noted how the π density slightly spreads toward the Me moiety, being redistributed in the HB3 zone, and increased around the O2 site, which can be attributed to a hyperconjugative effect. In fact, although the π system contributes to stabilize the HBs as it has been already observed in other compounds,[23] it is scarcely affected by the presence of the Me group. This stabilization effect can be interpreted taking into account that the interaction with the π system contributes to increase the attraction of the protons to the acceptor and/or donor atoms, as they are the source of the π(HB) system (for example, π(C−O2) and LP$_\pi$(N3), in the case of HB3).

In order to assess the effect of this redistribution of electronic density in the bridge area, Table 3 shows the monoelectronic

DOI: 10.1021/acs.jpca.6b10059
J. Phys. Chem. A 2017, 121, 2960−2970

Table 3. Monoelectronic Interaction Energy between the Proton and the Electrons of the Molecular Orbitals Involved in the Bridge and the C−H1/Me Moiety, $V_{H,e^-} = \langle i|V_{He^-}|i\rangle$, at the Equilibrium Distance in HB3, for Compounds I and II[a]

LMO	I	II	Δ_{II-I}[d]
π(C−O2)	−0.49279	−0.49282	−0.00003
LP$_\pi$(N3)	−0.84375	−0.84265	0.00110
N3−H3+S(N3)	−2.78943	−2.78916	0.00027
LP$_\sigma$(O2) (x2) + S(O2)	−1.70863	−1.70864	−0.00001
HB[b]	−5.83460	−5.83328	0.00132
C−H1/Me[c]	−0.63445	−1.68103	−1.04658

[a]All values in au. [b]Includes all LMOs of the HB moiety. [c]C−H1+S(C5) for compound I, and Me+S(C5) for compound II. [d]Note that a positive sign indicates larger interaction energy in compound I than in compound II, while a negative sign indicates the opposite trend.

Table 4. Comparison of the Potential Energy of Protons, at the Position of the Principal Minima, between Model Compounds I and II, and CG and C5meCG[a]

	I	II	CG	C5meCG
HB1	−0.39839	−0.99252	−0.37486	−0.96419
HB2	0.17102	−0.55673	0.16899	−0.52116
HB3	−0.58112	−1.62635	−0.58338	−1.62483

[a]All values in au.

interaction energy between the proton and the electrons of the molecular orbitals involved in the HB3 bridge,V_{H,e^-}, for the equilibrium distance. It is observed that the attraction among π and σ electrons of the donor moieties with the H proton slightly decreases, while the interaction with the electrons involved with the O2 acceptor is nearly not altered: only a very small increase is observed, compatibly with the slight increase of the electronic density about the O2, which is not large enough to counteract the effect of the Me group. As expected, the interaction between the Me group electrons and the proton is stronger than that of the C−H1 group and, as it was already shown, it accounts for almost the total potential energy difference between II and I.

In order to validate the used approach, the potential energy of protons, at the position of the principal minima, between model compounds I and II, and base pairs CG and C5meCG are compared in Table 4. It is interesting to note that similar molecular fragments lead to similar qualitative and almost quantitative trends, despite the differences in their environments.

Influence of the Me Group on the HB Polarizability. In the preceding section it is obtained that there is a stabilization effect of the HBs due to the presence of the Me group, which could be ascribed to the monoelectronic interaction energy among the proton and the electrons of the Me fragment. This effect was shown to alter the potential energy of the HB moieties, deepening the potential well and, therefore, further localizing the protons in the vicinity of the donor/acceptor atom closer to the Me moiety. This effect is more marked for HB3.

This feature can be rationalized taking into account that the electrons of the Me group not only interact with the proton, but there would be a transfer of these electrons toward the HB zone. This "delocalization" of the Me electrons is not evidenced either by the interaction energies or by Figure 4a,b, as it is screened by the redistribution of the HB electronic density itself. As it was found before,[23] this effect cannot be detected straightforwardly by means of a first-order property like the potential energy, but with a second-order property like proper and mutual polarizabilities. Therefore, an analysis of these properties is accomplished for HB3, as this HB is the most affected by the presence of the Me group.

In Table 5, RPA averaged in-plane $\langle\alpha_{xy}\rangle$, out of plane α_{zz}, and averaged total $\langle\alpha\rangle$ values of the polarizability tensors on model compounds I and II, and CG and C5meCG are displayed. SOPPA values are also shown for comparison, calculated with the DALTON program.[38] From this table, it can be seen that, although correlation effects are not negligible, RPA values follow the same trends as SOPPA ones. In fact, although underestimated, the relative values among all polarizabilities are well reproduced by RPA values when compared with SOPPA ones. Therefore, it can be concluded that RPA values are adequate for performing a qualitative analysis of these polarizabilities.

With regard to the values shown, RPA or SOPPA ones, it should be noted again that those corresponding to the model compounds can not be directly compared with those of the base pairs, although it is worthy to note again that the difference between values corresponding to the model compounds are practically the same as those corresponding to the base pairs. Moreover, it is observed that methylated compounds have larger polarizability values than the unmethylated ones. This fact cannot relate directly to a greater or lesser strength of the hydrogen bonds, as it has been pointed out in the literature[17,20] (although it can be related with their stacking ability,[17,24] because the whole environment of the bridges is involved in the polarizability. Therefore, to draw conclusions from this global upshot could be misinterpreting and it deserves further analysis. For that reason, it is most convenient to

Table 5. RPA and SOPPA Averaged In-Plane$\langle A_{xy}\rangle$, Out-of-Plane α_{zz}, and Averaged Total $\langle\alpha\rangle$ Values of the Polarizability Tensors on Model Compounds I and II, and CG and C5meCG[a]

	RPA			SOPPA		
	$\langle\alpha_{xy}\rangle$	α_{zz}	$\langle\alpha\rangle$	$\langle\alpha_{xy}\rangle$	α_{zz}	$\langle\alpha\rangle$
I	129.3938	36.0672	98.2849	152.5005	37.7034	114.2348
II	140.6398	45.3339	108.8711	164.3299	47.0041	125.2213
Δ_{II-I}	11.2460	9.2667	10.5862	11.8294	9.3007	10.9865
CG	168.3584	46.7513	127.8227	198.7073	49.1501	148.8549
C5meCG	179.6547	55.9793	138.4296	210.6201	58.4101	159.8834
$\Delta_{C5meCG-CG}$	11.8294	9.3007	10.9865	11.9128	9.2600	11.0285

[a]All values in au.

DOI: 10.1021/acs.jpca.6b10059
J. Phys. Chem. A 2017, 121, 2960−2970

perform an analysis taking into account the molecular fragments of interest, that is, the HB fragments.

In Table 6, the IPPP main components, the averaged in-plane value, and the averaged total value of the polarizability tensor for the molecular fragment HB3, in compounds I, II, CG, and C5meCG are displayed. For the fragment, the calculation was performed taking into account (i) the contribution of vacant and occupied HB3 LMOs plus the total, occupied, and vacant X (X = Me,C−H1) system, (ii) the contribution of vacant and occupied X (X = Me,C−H1) LMOs, and (iii) the difference between (i) and (ii). The latter includes the direct influence of the X group on the polarizability of the HB3 moiety, i.e.,

$$\alpha_\mu + \Delta\alpha_\mu = \sum_{ij}^{HB3} \alpha_{ij} + \sum_{i}^{HB3}\sum_{j}^{X} \alpha_{ij} \quad \mu = xx, yy, zz$$

where the α_{ij} terms are calculated taking into account HB3* and X* vacant LMOs. The first summation represents the proper polarizability of the HB3 fragment over the HB zone, while the second one gives the contribution of the Me/C−H1 group, that is, the mutual polarizability between the HB3 fragment and the X moiety. As the HB3 lays in the *xy*-plane, along the *x* direction, the in-plane averaged polarizability, and the *xx* and *yy* components as well, are analyzed in depth. From this table it can be seen that the in-plane averaged polarizability and the *xx* and *yy* components of the HB3 fragment are smaller in compound II than in I. The same qualitative and almost quantitative trend is observed for the corresponding values of C5meCG with respect to those of CG, showing again that the effect of methylation on the HBs is well reproduced by similar molecular fragments in the model compounds. This fact shows that the Me system contributes to decrease the polarizability of the hydrogen bond, that is, to decrease the mobility of the HB3 electrons in the HB and X zone. Further analysis can be made, so as to establish the effect of the Me system on the electronic distribution of the HB moiety. In order to understand how the Me system influences the polarizabilities of the HB LMOs, Tables 7 and 8 display the proper and mutual polarizabilities with the X group on the bridge, of the whole HB3 system (Table 7), each individual HB3 LMO with the X group, and the rest of the LMOs of the HB3 moiety (Table 8). Only the *xx* component of polarizabilities is shown, as this component is that which corresponds to the HB direction. In order to take into account the polarizability on the bridge zone, the subspace of vacant LMOs is restricted to only the HB* ones. From these tables, the values of proper and mutual polarizabilities are enlightening. In fact, it is interesting to observe that the presence of the Me group produces a drop of the proper polarizability of the HB3 fragment onto the HB region. The same trend is observed for all LMOs of the HB3 fragment, as it is depicted in Table 8. This characteristic shows that the Me group tends to further localize the electrons of the HB3 fragment, decreasing their mobility. On the contrary, the proper polarizabity of the Me moiety increases onto the same region, with respect to that of the C−H1 group. This suggests that the Me electrons are more likely to spread onto the bridge zone than the C−H1 ones, increasing in that way the interaction with the proton and, therefore, the corresponding interaction energy.

This behavior can be visualized if the interpretation of α_{ii} terms, eqs 8 and 9, is taken into account. In particular, by inspection of eq 9, the following rationalization can be made. The induced dipole of a given $|i\rangle$ LMO occurs when it is perturbed and connected to a vacant $|a^*\rangle$ LMO, that is, the virtual excitation $i \rightarrow a^*$ is produced. Hence, the vacant $|a^*\rangle$ LMO is partially occupied, and the perturbed orbital $|\tilde{i}\rangle$ shows how the $|i\rangle$ LMO is polarized over the region occupied by the $|a^*\rangle$ LMO, due to the perturbation. As a result, the mean electric field on nuclei and electrons occupying other LMOs is changed, and the distribution of electronic charge within the molecule is altered. In fact, the PP describes this internal change, thus determining the magnitude of the "response" $i \rightarrow a^*$. In the present case, this change can be explained on qualitative grounds. It is interesting to observe that as $|i\rangle$ = LMOs(X) (X = C−H1, Me) are connected with $|a^*\rangle$ = HB* vacant LMOs, it can be expected that this group of occupied LMOs becomes more spread over the whole bridge region (so much as the proper polarizabilty magnitude indicates). In fact, this feature can be observed in Figure 5, where the electronic

Table 6. IPPP Main Components, Averaged In-Plane $\langle\alpha_{xy}\rangle$, and Averaged Total $\langle\alpha\rangle$ Values of the Polarizability Tensors for the HB3 and the X = Me,C−H1 Groups on Model Compounds I and II, and CG and C5meCG[a]

	α_{xx}	α_{yy}	α_{zz}	$\langle\alpha_{xy}\rangle$	$\langle\alpha\rangle$
HB3 + X[b]					
I	6.2445	5.2658	3.7807	5.7551	5.0970
II	9.5961	8.3771	5.2559	8.9866	7.7430
CG	6.1672	6.0825	3.8256	6.1248	5.3584
C5meCG	9.0332	8.5852	4.5721	8.8092	7.3968
X[c]					
I	1.5577	2.1490	0.0006	1.8533	1.2358
II	5.0606	5.4397	1.3867	5.2501	3.9623
CG	1.5571	2.1465	0.0006	1.8518	1.2347
C5meCG	4.4245	5.0607	0.8364	4.7426	3.4041
$\alpha + \Delta\alpha$[d]					
I	4.6868	3.1168	3.7801	3.9018	3.8612
II	4.5355	2.9374	3.8692	3.7365	3.7807
CG	4.6101	3.9360	3.8250	4.2730	4.1237
C5meCG	4.6087	3.5245	3.7357	4.066	3.9927

[a]All values in au. [b]It includes HB and X occupied and vacant LMOs. X = Me for compounds I and CG; X = C−H1 for compounds II and C5meCG. [c]It includes X occupied and vacant LMOs. [d]$\alpha+\Delta\alpha$ indicates the difference between (HB3+X) and X. See text for explanation.

Table 7. IPPP *xx* Component of Proper and Mutual HB3 Polarizabilities, α_{xx}, in Model Compounds I and II, and CG and C5meCG, for HB and X = Me,C−H1 Moieties[a]

LMOs[b]	LMO*s[c]	I	II	Δ_{II-I}
HB	HB*	4.6136	4.3499	−0.2637
X	HB*	0.1004	0.3382	0.2378
HB/X	HB*	0.0044	0.0154	0.0110
LMOs[b]	LMO*s[c]	CG	C5meCG	$\Delta_{C5meCG-CG}$
HB	HB*	4.5413	4.4449	−0.0964
X	HB*	0.0990	0.3978	0.2988
HB/X	HB*	0.0041	0.0177	0.0136

[a]All values in au. X = C−H1 for compounds I and CG; X = Me for compounds II and C5meCG. [b]Y (Y = HB,X) indicates proper polarizability of the fragment Y: $\alpha_{YY} = \sum_i^Y \sum_j^Y \alpha_{ij}$. Y/X indicates mutual polarizability between fragments Y and X:$\alpha_{YX} = \sum_i^Y \sum_j^X \alpha_{ij}$. [c]The symbol '*' indicates vacant LMOs.

DOI: 10.1021/acs.jpca.6b10059
J. Phys. Chem. A 2017, 121, 2960−2970

Table 8. IPPP *xx* Component, α_{xx}, of Proper and Mutual Polarizabilities with the X = Me,C−H1 Moieties, of the Main LMOs of the HB3 Fragment over the HB Zone, in Model Compounds I and II[a]

LMO(1)	LMO(2)	I	II	Δ_{II-I}
N3−H3	N3−H3	1.0636	1.0575	−0.0061
	HB[b]	0.1527	0.1449	−0.0078
	X	0.0019	0.0052	0.0034
$LP_\sigma(O2)$[c]	$LP_\sigma(O2)$	1.7229	1.7121	−0.0108
	HB[b]	−0.0100	0.0844	0.0944
	X	0.0011	0.0035	0.0024
$LP_\pi(N3)$	$LP_\pi(N3)$	0.7267	0.6059	−0.1208
	HB[b]	0.0344	0.0346	0.0002
	X	0.0009	0.0053	0.0044
π(C−O2)	π(C−O2)	1.0753	0.8593	−0.2160
	HB[b]	−0.1270	−0.0407	−0.0863
	X	0.0005	0.0013	0.0008

[a]All values in au. Proper and mutual polarizabilities are calculated taking into account HB* vacant LMOs. X = C−H1 for compound I; X = Me for compound II. [b]LMO(2) = HB represents the rest of occupied LMOs of the HB3 moiety other than LMO(1). [c]It includes both $LP_\sigma(O2)$.

density of (a) perturbed Me in compound II, (b) C−H1 in compound I onto the HB region, and (c) the difference between a and b is depicted. It is noteworthy that Me perturbed LMOs tend to spread more than the C−H1 one over the N3−H3 zone, and a little less around the O2, as it can be observed in Figure 5c. As a consequence, the electric field in the bridge zone due to the X group changes its intensity and, therefore, alters the charge distribution. Figure 6 shows this electric field change for both compounds I and II. It is noteworthy that the perturbed Me electric field changes in such a way that favors the flow of electrons toward the surroundings of the N3, unlike the C−H1 one, which favors a decrease of the electronic density around this nucleus site. However, this is not the only difference between them. In fact, whereas the electric field of the C−H1 group is scarcely and uniformly altered, the Me group electric field presents significant changes, the main one being that it increases its (negative) intensity in the whole N3−H3 zone. Therefore, the interaction with the bridge proton is increased, and this leads to a major localization of the proton in the proximity of N3. Hence, this fact explains the effect of stabilization of the HB due to the presence of the Me group, when compared with the C−H1 one, as it was pointed out before.

A similar analysis can be performed taking into account the drop of proper polarizabilities of HB3 LMOs, due to the presence of the Me group. Figure 7 depicts the difference between (a) σ, $\Delta\tilde{\rho}_\sigma$, and (b) π, $\Delta\tilde{\rho}_\pi$ contributions of HB* vacant LMOs to the electronic densities of perturbed HB3 LMOs, between compounds II and I (π electronic densities are calculated at 0.5 au from the molecular plane). As it was mentioned before, Figure 7 shows how the presence of the Me

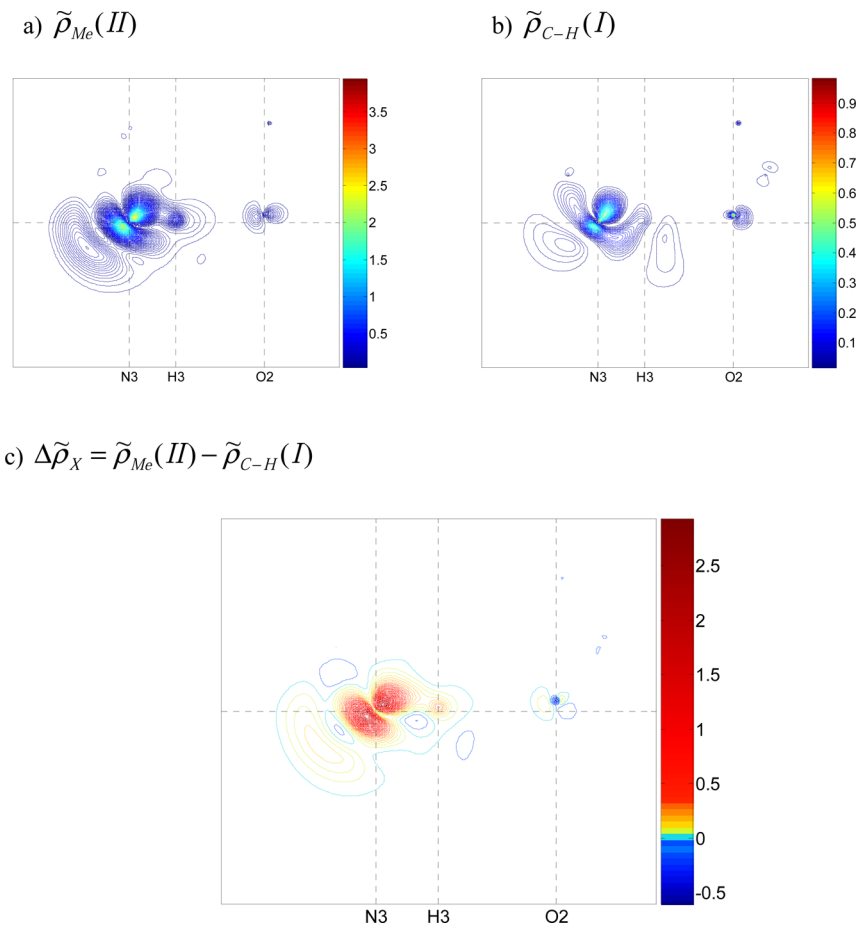

Figure 5. Contribution of the HB* vacant LMOs to the electronic density of X perturbed LMOs, $\tilde{\rho}_X$, between compounds II and I, and the difference between them, $\Delta\tilde{\rho}_X$.

DOI: 10.1021/acs.jpca.6b10059
J. Phys. Chem. A 2017, 121, 2960−2970

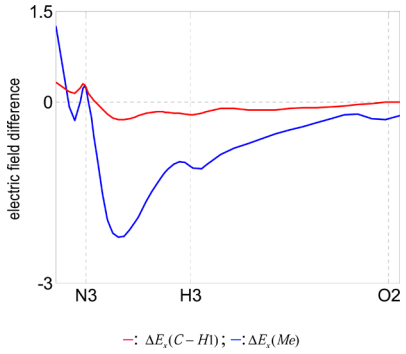

Figure 6. Plot of the electric field change (in au) of the X group (X = Me, C−H1) as it is perturbed and connected with the HB* vacant LMOs.

a) $\Delta\tilde{\rho}_\sigma = \tilde{\rho}_\sigma(II) - \tilde{\rho}_\sigma(I)$

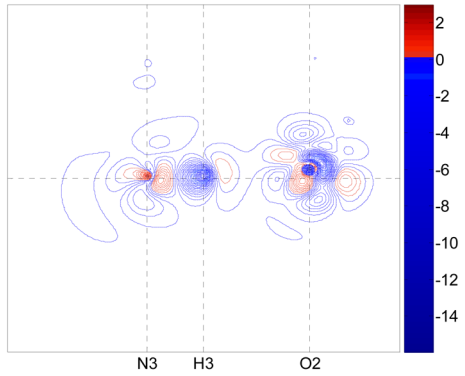

b) $\Delta\tilde{\rho}_\pi = \tilde{\rho}_\pi(II) - \tilde{\rho}_\pi(I)$

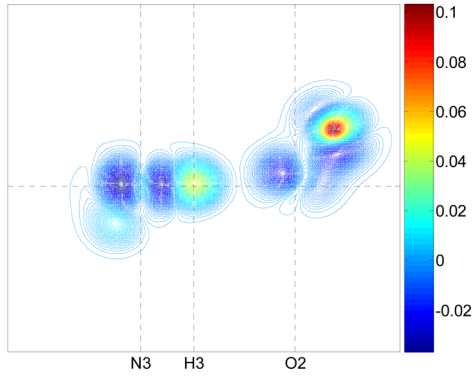

Figure 7. Difference between (a) σ, $\Delta\tilde{\rho}_\sigma$ and (b) π, $\Delta\tilde{\rho}_\pi$ contributions of HB* vacant LMOs to the electronic densities of perturbed HB3 LMOs, between compounds II and I. π electronic densities are calculated at 0.5 au from the molecular plane.

group tends to localize the σ-electrons of the HB region at the site of the donor and acceptor atoms, thus reducing their mobility, unlike the C−H1 bond, for which the effect is much less significant. As compounds II and I differ only in the X group, the difference between perturbed LMOs in II and I seems to be only due to the different electric field of X in both compounds (Figure 6). In fact, the highly negative electric field of the perturbed Me LMOs tends to further confine the electrons around their positive centers, and therefore, to reduce its mobility.

Finally, as far as mutual polarizabilities α_{ij}^{rs} $(i \neq j;\ r,s = x,y,z)$ are concerned, they carry information about interactions between the electronic distribution of $|i\rangle$ and $|j\rangle$ LMOs.[23,26,27] Thus, the magnitude of mutual polarizabilities α_{ij}^{rs} depends on the extent to which the two LMOs involved are polarizable,[23,27] and its sign indicates whether the dipole moment induced in the $|i\rangle$ LMO, due to the field produced by the induced dipole moment on the $|j\rangle$ LMO, is parallel (positive) or antiparallel (negative) to that produced by the external field.[23,27] In this case, it is interesting to note that, although proper HB3 polarizabilities decrease by the presence of the Me fragment, mutual polarizabilities with this group, although very small, increase as compared with that of the C−H1 group. This can be thought of as only due to the Me group being more polarizable than the C−H1 one, since the HB LMOs are less polarizable due to the effect of the induced dipole field of the Me group on the electrons of the HB region. On the contrary, mutual polarizabilities between HB3 LMOs decrease for the methylated compound, a fact that confirms again that the interaction with the Me electronic system tends to produce a major localization of the electrons of the HB moiety. Extreme examples are those of the mutual polarizabilities $LP_\sigma(O2)/HB$ and $\pi(C{-}O2)/HB$. The former changes sign, being negative for I and positive for II. By inspection of this term, it is noted that the change of sign is mainly due to the mutual polarizability between $LP_\sigma(O2)$ and $\pi(C{-}O2)$, which changes from −0.1756 au for I to −0.0792 au for II. These terms show that even the π system is more localized due to its interaction with the Me group. In this case, the negative sign of these terms would indicate that the two LMOs share a region in space where they are nearly parallel.

CONCLUSIONS

In the present study, the influence of the Me group on the energy and the potential energy curve of the protons of the intermolecular hydrogen bonds of model compounds that mimic the methylated and unmethylated cytosine-guanine base pair (C5mCG and CG, respectively) are analyzed by means of the IPPP-CLOPPA method. This influence on the electric dipolar molecular polarizability of the HBs is also evaluated. The focus was put on whether the analysis of these properties provides a clue of the electronic mechanisms that lead to the increased strength of the methylated compounds when compared with the unmethylated ones. Results obtained are compared with the corresponding values calculated for the CG and C5mCG bases pairs in order to validate the performed analysis and to show how similar molecular fragments lead to similar qualitative and quantitative trends.

The analysis of the potential energy of the proton in the HB moieties shows that the interaction of the Me system with the protons yields significant changes in the potential energy, increasing the depth of the potential wells that are closer to the Me group and, therefore, making them more asymmetrical. These effects are evidence of an actual strengthening of the HBs due to the presence of the Me electrons in the HB environment. In fact, it was found out that this stabilization effect is due to the monoelectronic interaction energy between the proton and the electrons of the Me fragment, rather than a change of the interaction with the proper electrons of the HB zone.

DOI: 10.1021/acs.jpca.6b10059
J. Phys. Chem. A 2017, 121, 2960−2970

The preceding results are highlighted in depth with the analysis of the molecular polarizability of the HB fragment. With respect to the total value of each component of the polarizability tensor of the fragment, they do not reflect any evidence of a singular influence of the Me system on the hydrogen bond moiety, or any sign that could be attributed to an interaction between delocalized-onto-the HB-zone electrons of the Me group and proper electrons of the HB LMOs. However, as it was found before,[23] considering the bulk property would be misleading and conveys conclusions that could be misunderstood. So, results require a further analysis. In fact, it is demonstrated[23] that an in-depth analysis by decomposing the total polarizability in proper and mutual values leads to a qualitative and quantitative description of interactions in the HB zone. Thus, for example, it is interesting to observe that the presence of the Me group produces a drop of the proper polarizability of the total HB3 fragment onto the HB region, and the same follows for all the HB3 LMOs. This characteristic shows that the Me group tends to localize more the electrons of this hydrogen bond fragment, reducing their mobility. On the contrary, the proper polarizabity of the Me moiety increases onto the same region, with respect to that of the C−H1 group. This evidences that the Me electrons are more likely to spread onto the bridge zone than the C−H1 ones, which finally changes its electric field onto the HB zone.

To summarize, the presented results lead to the conclusion that the hydrogen bonds of the methylated compound are actually strengthened by their interaction with the Me group, as it is shown that (a) the electrons of Me system tend to delocalize within the HB fragment and, therefore, this effect, in fact, alters the charge distribution and the electric field onto the bridge zone, and (b) as a consequence, there is an intense interaction of the Me electronic system with the HB protons, which leads to a major localization of the proton in the proximity of its donor atom. This effect actually contributes to the strength of the hydrogen bonds, as it can be observed from the potential energy curves. Hence, this fact explains the effect of stabilization of the HB due to the presence of the Me group, when compared with the C−H1 one.

AUTHOR INFORMATION

Corresponding Author

*E-mail: giribet@df.uba.ar.

ORCID

Claudia G. Giribet: 0000-0002-3661-1693

Notes

The authors declare no competing financial interest.

ACKNOWLEDGMENTS

This paper is dedicated to the loving memory of Martín Ruiz de Azúa, my husband, my partner in life and research, who passed away in 2014. I will love him and miss him forever. Financial support from UBACYT and CONICET is gratefully acknowledged.

REFERENCES

(1) Ebrahimi, A.; Habibi Khorassani, S. M.; Delarami, H.; Esmaeeli, H. The Effect of CH3, F and NO2 Substituents on the Individual Hydrogen Bond Energies in the Adenine−Thymine and Guanine−Cytosine Base Pairs. *J. Comput.-Aided Mol. Des.* **2010**, *24*, 409−416.

(2) Clementi, E.; Mehl, J.; Von Niessen, W. Study of the Electronic Structure of Molecules. XII. Hydrogen Bridges in the Guanine−Cytosine Pair and in the Dimeric Form of Formic Acid. *J. Chem. Phys.* **1971**, *54*, 508.

(3) Rein, R.; Harris, F. E. Studies of Hydrogen-Bonded Systems. I. The Electronic Structure and the Double Well Potential of the N-H.. · N Hydrogen Bond of the Guanine-Cytosine Base Pair. *J. Chem. Phys.* **1964**, *41*, 3393.

(4) Löwdin, P.-O. Proton Tunneling in DNA and its Biological Implications. *Rev. Mod. Phys.* **1963**, *35*, 724.

(5) Vanyushin, B. F. Enzymatic DNA Methylation Is an Epigenetic Control for Genetic Functions of the Cell. *Biochemistry (Moscow)* **2005**, *70*, 488−499.

(6) Vanyushin, B. F. A View of an Elemental Naturalist at the DNA World (Base Composition, Sequences, Methylation). *Biochemistry (Moscow)* **2007**, *72*, 1289−1298.

(7) Forde, G.; Flood, A.; Salter, L.; Hill, G.; Gorb, L.; Leszczynski, J. Theoretical ab Initio Study of the Effects of Methylation on Structure and Stability of G:C Watson-Crick Base Pair. *J. Biomol. Struct. Dyn.* **2003**, *20*, 811−817.

(8) Si, X.; Zhao, Y.; Yang, C.; Zhang, S.; Zhang, X. DNA Methylation as a Potential Diagnosis Indicator for Rapid Discrimination of Rare Cancer Cells and Normal Cells. *Sci. Rep.* **2015**, *5*, 11882.

(9) Song, Q.; Qiu, Z.; Wang, H.; Xia, Y.; Shen, J.; Zhang, Y. The Effect of Methylation on the Hydrogen-Bonding and Stacking Interaction of Nucleic Acid Bases. *Struct. Chem.* **2013**, *24*, 55−65.

(10) Phillips, T. The Role of Methylation in Gene Expression. *Nature Education* **2008**, *1*, 116−121.

(11) Dantas Machado, A. C.; Zhou, T.; Rao, S.; Goel, P.; Rastogi, C.; Lazarovici, A.; Bussemaker, H. J.; Rohs, R. Evolving Insights on How Cytosine Methylation Affects Protein-DNA Binding. *Briefings Funct. Genomics* **2015**, *14*, 1−13.

(12) Severin, P. M. D.; Zou, X.; Gaub, H. E.; Schulten, K. Cytosine Methylation Alters DNA Mechanical Properties. *Nucleic Acids Res.* **2011**, *39*, 8740−8751.

(13) Demokan, S.; Dalay, N. Role of DNA Methylation in Head and Neck Cancer. *Clin. Epigenet.* **2011**, *2*, 123−150.

(14) Thienpont, B.; Steinbacher, J.; Zhao, H.; D'Anna, F.; Kuchnio, A.; Ploumakis, A.; Ghesquière, B.; Van Dyck, L.; Boeckx, B.; Schoonjans, L.; Hermans, E.; Amant, F.; Kristensen, V.; Koh, K. P.; Mazzone, M.; Coleman, M. L.; Carell, T.; Carmeliet, P.; Lambrechts, D. Tumour Hypoxia Causes DNA Hypermethylation by Reducing TET Activity. *Nature* **2016**, *537*, 63−68.

(15) Bergman, Y.; Cedar, H. DNA Methylation Dynamics in Health and Disease. *Nat. Struct. Mol. Biol.* **2013**, *20*, 274−281.

(16) Mirsaidov, U.; Timp, W.; Zou, X.; Dimitrov, V.; Schulten, K.; Feinberg, A. P.; Timp, G. Nanoelectromechanics of Methylated DNA in a Synthetic Nanopore. *Biophys. J.* **2009**, *96*, 32−34.

(17) Moser, A.; Guza, R.; Tretyakova, R.; York, D. M. Density Functional Study of the Influence of C5 Cytosine Substitution in Base Pairs with Guanine. *Theor. Chem. Acc.* **2009**, *122*, 179−188.

(18) Yusufaly, T. I.; Li, Y.; Olson, W. K. 5-Methylation of Cytosine in CG:CG Base-pair Steps: A Physicochemical Mechanism for the Epigenetic Control of DNA Nanomechanics. *J. Phys. Chem. B* **2013**, *117*, 16436−16442.

(19) Flood, A.; Hubbard, C.; Forde, G.; Hill, G.; Gorb, L.; Leszczynski, J. Theoretical Ab Initio Study of the Effects of Methylation on the Nature of Hydrogen Bonding in A:T Base Pair. *J. Biomol. Struct. Dyn.* **2003**, *21*, 297−302.

(20) Sponer, J.; Leszczynski, J.; Hobza, P. Electronic Properties, Hydrogen Bonding, Stacking, and Cation Binding of DNA and RNA Bases. *Biopolymers* **2001**, *61*, 3−31.

(21) Sponer, J.; Jurecka, P.; Hobza, P. Accurate Interaction Energies of Hydrogen-Bonded Nucleic Acid Base Pairs. *J. Am. Chem. Soc.* **2004**, *126*, 10142−10151.

(22) Smith, Q. A.; Gordon, M. S.; Slipchenko, L. V. Effective Fragment Potential Study of the Interaction of DNA Bases. *J. Phys. Chem. A* **2011**, *115*, 11269−11276.

(23) Giribet, C. G.; Ruiz de Azúa, M. C. CLOPPA Analysis of the Molecular Polarizability and the Energy of Strong Intramolecular

DOI: 10.1021/acs.jpca.6b10059
J. Phys. Chem. A 2017, 121, 2960−2970

Hydrogen Bonds: Resonance Assisted? *J. Phys. Chem. A* **2012**, *116*, 12175−12183.
(24) Xiao, S.; Wang, L.; Liu, Y.; Lin, X.; Liang, H. Theoretical Investigation of the Proton Transfer Mechanism in Guanine-Cytosine and Adenine-Thymine Base Pairs. *J. Chem. Phys.* **2012**, *137*, 195101−195108.
(25) Sowers, L. C.; Shaw, B. R.; Sedwick, W. D. Base Stacking and Molecular Polarizability: Effect of a Methyl Group in the 5-Position of Pyrimidines. *Biochem. Biophys. Res. Commun.* **1987**, *148*, 790−794.
(26) Giribet, C. G.; Demarco, M. D.; Ruiz de Azúa, M. C.; Contreras, R. H. *Ab-initio* CLOPPA Decomposition of the Static Molecular Polarizability Tensor. *Mol. Phys.* **1997**, *91*, 105−112.
(27) Botek, E. L.; Giribet, C. G.; Ruiz de Azúa, M. C.; Negri, R. M.; Bernik, D. Evaluation of the Molecular Polarizability Using the IPPP-CLOPPA-INDO/S Method. Application to Molecules of Biological Interest. *J. Phys. Chem. A* **2008**, *112*, 6992−6998.
(28) Giribet, C. G.; Ruiz de Azúa, M. C. CLOPPA-IPPP Analysis of Cooperative Effects in H-bonded Molecular Complexes.2. Application to the Static Molecular Polarizability Tensor. *J. Phys. Chem. A* **2010**, *114*, 1109−1117.
(29) Ruiz de Azúa, M. C.; Diz, A. C.; Giribet, C. G.; Contreras, R. H.; Rae, I. D. A Polarization Propagator Analysis of Through-Space Spin-Spin Coupling Constants: F-F Couplings. *Int. J. Quantum Chem.* **1986**, *30*, 585−601.
(30) Diz, A. C.; Giribet, C. G.; Ruiz de Azúa, M. C.; Contreras, R. H. The Use of Localized Molecular Orbitals and the Polarization Propagator Approach to Identify Transmission Mechanisms in Nuclear Spin-Spin Couplings. *Int. J. Quantum Chem.* **1990**, *37*, 663−677.
(31) Ruiz de Azúa, M. C.; Giribet, C. G.; Vizioli, C. V.; Contreras, R. H. *Ab-initio* IPPP-CLOPPA Approach to Perform Bond Contribution Analysis of NMR Coupling Constants: $^{1}J(NH)$ in NH_3 as a Function of Pyramidality. *J. Mol. Struct.: THEOCHEM* **1998**, *433*, 141−150.
(32) Giribet, C. G.; Ruiz de Azúa, M. C.; Vizioli, C. V.; Cavasotto, C. N. Electronic Mechanisms of Intra and Intermolecular J Couplings in Systems with C-H···O Interactions. *Int. J. Mol. Sci.* **2003**, *4*, 203−217.
(33) Contreras, R. H.; Peralta, J. E.; Giribet, C. G.; Ruiz de Azúa, M. C.; Facelli, J. C. Advances in Theoretical and Physical Aspects of Spin−Spin Coupling Constants. In *Annual Reports on NMR Spectroscopy*, Elsevier Inc.: London/San Diego, 2000; Vol. *41*, pp 57−166.
(34) Giribet, C. G.; Ruiz de Azúa, M. C. CLOPPA-IPPP Analysis of Electronic Mechanisms of Intermolecular $^{1h}J(A,H)$ and $^{2h}J(A,D)$ Spin-Spin Coupling Constants in Systems with D-H···A Hydrogen Bonds. *J. Phys. Chem. A* **2005**, *109*, 11980−11988.
(35) Giribet, C. G.; Ruiz de Azúa, M. C. The Sign and Magnitude of $^{2h}J(F,F)$ and $^{1h}J(F,H)$ in FH···FH. A CLOPPA Analysis of their Distance Dependence. *J. Phys. Chem. A* **2006**, *110*, 11575−11583.
(36) Giribet, C. G.; Ruiz de Azúa, M. C. CLOPPA-IPPP Analysis of Cooperative Effects in H-bonded Molecular Complexes. Application to Intermolecular $^{2h}J(N,C)$ Spin-Spin Coupling Constants in Linear $(CNH)_n$ Complexes. *J. Phys. Chem. A* **2008**, *112*, 4386−4393.
(37) Jørgensen, P.; Simons, J. In *Second Quantization based Methods in Quantum Chemistry*; Academic Press: London, 1981.
(38) Aidas, K.; Angeli, C.; Bak, K. L.; Bakken, V.; Bast, R.; Boman, L.; Christiansen, O.; Cimiraglia, R.; Coriani, S.; Dahle, P.; Dalskov, E. K.; Ekström, U.; Enevoldsen, T.; Eriksen, J. J.; Ettenhuber, P.; Fernández, B.; Ferrighi, L.; Fliegl, H.; Frediani, L.; Hald, K.; Halkier, A.; Hättig, C.; Heiberg, H.; Helgaker, T.; Hennum, A. C.; Hettema, H.; Hjertenæs, E.; Høst, S.; Høyvik, I.-M.; Iozzi, M. F.; Jansik, B.; Jensen, H. J.; Aa; Jonsson, D.; Jørgensen, P.; Kauczor, J.; Kirpekar, S.; Kjærgaard, T.; Klopper, W.; Knecht, S.; Kobayashi, R.; Koch, H.; Kongsted, J.; Krapp, A.; Kristensen, K.; Ligabue, A.; Lutnæs, O. B.; Melo, J. I.; Mikkelsen, K. V.; Myhre, R. H.; Neiss, C.; Nielsen, C. B.; Norman, P.; Olsen, J.; Olsen, J. M. H.; Osted, A.; Packer, M. J.; Pawlowski, F.; Pedersen, T. B.; Provasi, P. F.; Reine, S.; Rinkevicius, Z.; Ruden, T. A.; Ruud, K.; Rybkin, V.; Salek, P.; Samson, C. C. M.; Sánchez de Merás, A.; Saue, T.; Sauer, S. P. A.; Schimmelpfennig, B.; Sneskov, K.; Steindal, A. H.; Sylvester-Hvid, K. O.; Taylor, P. R.; Teale, A. M.; Tellgren, E. I.; Tew, D. P.; Thorvaldsen, A. J.; Thøgersen, L.; Vahtras, O.; Watson, M. A.; Wilson, D. J. D.; Ziolkowski, M.; Ågren, H. "The Dalton quantum chemistry program system". *WIREs Comput. Mol. Sci.* **2014**, *4*, 269−284.
(39) Van Duijneveldt-Van de Rijdt, J. G. C. M.; Van Duijneveldt, F. B. *J. Am. Chem. Soc.* **1971**, *93*, 5644.
(40) Lazzeretti, P.; Zanasi, R. Anisotropy of the Nuclear Spin−Spin Coupling Tensor in Water, Ammonia, and Methane Molecules. *J. Chem. Phys.* **1982**, *77*, 2448−2453.
(41) Lazzeretti, P. Geometric Approximation to Nuclear Spin−Spin Coupling Constants in the Water Molecule. *Int. J. Quantum Chem.* **1979**, *15*, 181−196.
(42) Lazzeretti, P. Calculation of Nuclear Spin−Spin Coupling Constants in Methanol Molecule. *J. Chem. Phys.* **1979**, *71*, 2514−2521.
(43) Jørgensen, P.; Simons, J. In *Second Quantization-based Methods in Quantum Chemistry*; Academic Press: London, 1981.
(44) Gilli, P.; Bertolasi, V.; Ferretti, V.; Gilli, G. Evidence for Intramolecular N−H···O Resonance-Assisted Hydrogen Bonding in β-Enaminones and Related Heterodienes. A Combined Crystal-Structural, IR and NMR Spectroscopic, and Quantum-Mechanical Investigation. *J. Am. Chem. Soc.* **2000**, *122*, 10405−10417.

DOI: 10.1021/acs.jpca.6b10059
J. Phys. Chem. A 2017, 121, 2960−2970